Detection of template binding to molecularly imprinted polymers by Raman microspectroscopy

Keren Kantarovich,[1] Anne-Sophie Belmont,[2,a)] Karsten Haupt,[2] Ilana Bar,[1] and Levi A. Gheber[3,b)]
[1]*Department of Physics, Ben-Gurion University of the Negev, Beer-Sheva 84105, Israel*
[2]*Compiègne University of Technology, UMR CNRS 6022, 60205 Compiegne, France*
[3]*Department of Biotechnology Engineering, Ben-Gurion University of the Negev, Beer-Sheva 84105, Israel*

(Received 18 January 2009; accepted 13 April 2009; published online 14 May 2009)

We report on sensitive and specific detection and quantification of a template in a molecularly imprinted polymer (MIP) using Raman microspectroscopy. The β-blocking drug *S*-propranolol and its enantiomer, *R*-propranolol, were used as target molecules since the selectivity of this MIP is well established and serves as an appropriate validation standard. Specific peaks originating in the template were identified in the Raman spectrum, allowing quantification of bound target molecule. We demonstrate that label-free monitoring can be achieved from volumes as small as 1 μm^3 of MIP, based on a single identifying peak. © *2009 American Institute of Physics*.
[DOI: 10.1063/1.3132061]

Molecularly imprinted polymers (MIPs) are synthetic receptors obtained by polymerization of suitable functional and cross-linking monomers around molecular templates.[1–3] The higher physical and chemical stability relative to biomacromolecules make MIPs potentially very suitable as recognition elements for chemical sensors, biosensors, or biochips.[4] Recently, a strong trend goes toward microbiochips—arrays of micrometer dots of biological molecules,[5,6] which have a great potential for applications in the bioanalytical field, drug development, environmental, food analysis, etc.[7,8]

To obtain MIP microarrays, we have previously demonstrated the deposition of microdroplets of MIP solution using microcantilevers or a nanofountain pen[9,10] and detection of specific binding of fluorescent target analytes. While this proved the feasibility of the patterning approach, this system is limited to detection of fluorescent targets.

A sensitive, label-free reporting method would represent a great advance toward portable arrayed sensors, consisting of small detection spots with high stability and label-free continuous monitoring. Standard label-free techniques such as (imaging) surface plasmon resonance or quartz crystal microbalance are nonspecific (they merely report the accumulation of material on the sensor surface) and lack the required spatial resolution. Other techniques that could be used for specific and quantitative label-free detection are infrared (IR) or Raman spectroscopies, which provide high chemical and structural information content. Nevertheless, both IR and Raman measurements have only scantly been demonstrated for MIPs analysis.[11–14] Raman microspectroscopy is expected to be particularly suitable since it combines the finger printing advantage of IR spectroscopy with the ease of use (no sample preparation) and high spatial resolution. Nevertheless, no quantitative and selective measurements of target binding have been reported so far.

Here we describe the use of Raman microspectroscopy for the detection and quantification of target molecules in very small volumes of MIP samples on solid surfaces. As a model analyte, we chose the chiral β-blocking drug *S*-propranolol. The *R*-enantiomer was used as the imprinting template, whereas the *S*-enantiomer is the ideal control compound, allowing to assess both sensitivity and selectivity of the system. The propranolol MIP has been previously described and characterized in great detail,[15] thus is an excellent candidate for comparison with our detection method.

Trimethylolpropane trimethacrylate (TRIM), methacrylic acid (MAA), diethyleneglycol dimethylether (diglyme), poly(vinyl acetate) (PVAc, molecular weight =140 000 g/mole), *S*-propranolol HCl, *R*-propranolol HCl and ^{3}H-*R*, *S*-propranolol were obtained from Sigma-Aldrich. 2,2-dimethoxy-2-phenyl acetophenone (DPAP) was from Fluka and the polished glass microscope slides from Hellma. The hydrochlorides of the propranolol enantiomers were converted into the corresponding free bases by extraction from a sodium carbonate solution at *p*H9 into chloroform.

The MIPs were synthesized by UV photopolymerization from a mixture containing TRIM (0.0964 mmol), MAA (0.0964 mmol), *R*-propranolol (0.0192 mmol), DPAP (0.0195 mmol), and 0.168 ml diglyme containing 2% PVAc. The cross-linker:monomer ratio was 1:1, and the monomer:template ratio was 5:1. A corresponding nonimprinted control polymer (NIP) was synthesized in the absence of the propranolol template. MIPs and NIPs were mechanically ground to 1–10 μm particles. The template was

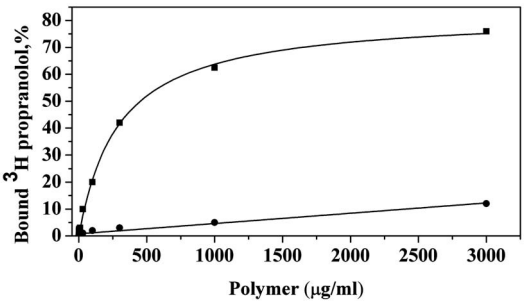

FIG. 1. Binding of ^{3}H-propranolol to imprinted (solid squares) and nonimprinted (solid circles) bulk polymers. Binding to MIP shows a Langmuir-like behavior while binding to NIP is weak and nonspecific.

a)Present address: Laboratoire des acides nucléiques, CEA Grenoble, France.
b)Electronic mail: glevi@bgu.ac.il.

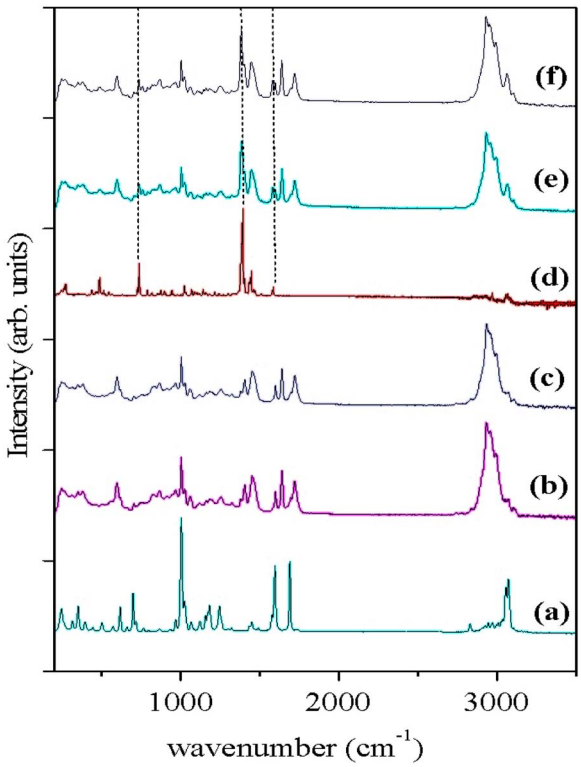

FIG. 2. (Color online) Raman spectra of DPAP (a), TRIM and MAA (b), monomers and porogen (c), *R*-propranolol (d), monomers and *R*-propranolol (e), monomers, *R*-propranolol, and porogen (f). The vertical dashed lines indicate the peaks related to the *R*-propranolol.

eluted by repeated incubation in ethanol/acetic acid 9:1 followed by two incubations in ethanol.

We have slightly altered the initial recipe by Andersson[15] describing the molecular imprinting of propranolol. Diglyme was used as porogenic solvent for its low vapor pressure to minimize evaporation that could occur in future fabrication of small MIP structures, similarly to our previously reported approach.[9] PVAc was added as a coporogen to accelerate pore formation since fast photopolymerization of small MIP structures yields nonporous material with a very low target binding capacity.[9,16] Since this porogen system is somewhat less favorable for the imprinting efficiency than toluene as

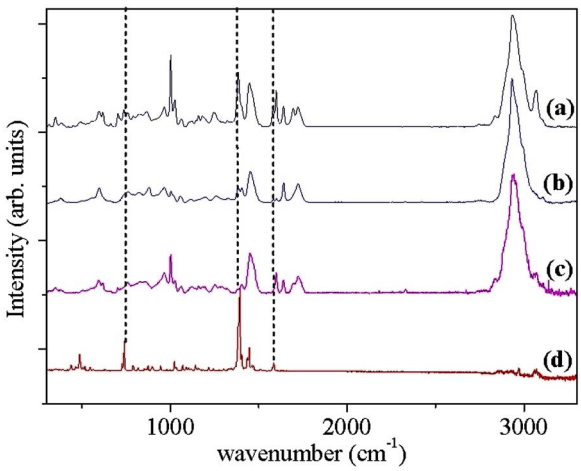

FIG. 3. (Color online) Normalized Raman spectra of MIP before (a) and after template extraction (b), a nonimprinted control polymer (c), and *R*-propranolol (d). The vertical dashed lines indicate the peaks related to *R*-propranolol, which decreased after template extraction.

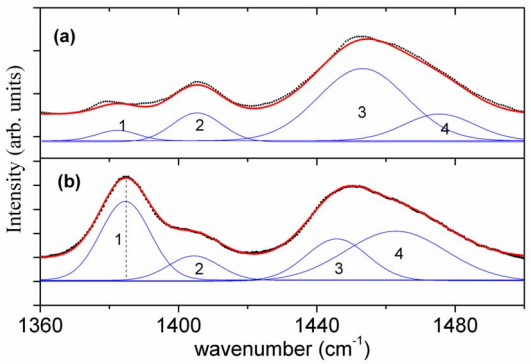

FIG. 4. (Color online) Deconvolution of the peak in the 1380 cm^{-1} region for (a) NIP and (b) MIP. The blue traces (1–4) show the four Gaussians used to obtain the fitted curve. The black dots and red lines represent the measured and fitted spectra, respectively. The dashed line indicates the peak used to quantify *R*-propranolol presence.

used by Andersson,[15] the amount of template in the mixture was increased and TRIM was used as cross-linker to maximize the number of binding sites, yielding a good compromise.

To verify the molecular imprinting of the polymers, the binding of radiolabeled propranolol by the MIP and the NIP control polymer was evaluated. Figure 1 shows the binding isotherm of an *R*-propranolol imprinted polymer. The MIP adsorbs the radioligand at relatively low polymer concentrations, whereas the NIP control shows only weak nonspecific binding at higher polymer concentrations, confirming molecular imprinting in the MIP. The binding capacity seems to be lower and the nonspecific binding slightly higher than those of the original polymers synthesized by Andersson[15] due to the different porogens used.

For Raman measurements, the MIP and NIP were incubated in a series of propranolol solutions in toluene at different concentrations for 3 h. The solutions were centrifuged at 11 000 rpm for 4 min, then the supernatant was removed from the Eppendorf tube and the powder was allowed to dry. MIP and NIP constituents were applied as drops (MAA and TRIM) or powder (DPAP, propranolol, and PVAC) on gold coated glass microscope slides.

Raman spectra were collected with a micro-Raman spectrometer (LabRam UV HR, Jobin-Yvon). The 784.9 nm excitation wavelength of a diode laser was focused onto the sample with an $\times 50/0.75$ numerical aperture objective, with ~ 10 mW intensity. The scattered light was redirected from the microscope through a sharp edge long wavepass filter that rejected the excitation laser line and through a confocal pinhole. This allowed rejection of out-of-focus signal, thus increasing detection sensitivity. The scattered light was focused into a 0.8 m dispersive spectrometer, equipped with a 600 groove/mm grating, and detected with a charge coupled device, consisting of 1024×256 pixels. Spectra were measured from at least five different points of each sample.

Initially the spectra of the MIP components were monitored to obtain characteristic "fingerprints" for their identification. Figure 2 presents the spectra obtained for DPAP (a), TRIM and MAA (b), TRIM, MAA, and PVAc in diglyme (c), *R*-propranolol (the template) (d), TRIM, MAA, and *R*-propranolol (e), and all the components: TRIM, MAA, *R*-propranolol, PVAc in diglyme (f). Comparison of these spectra allows to easily identify the peaks contributed by the template molecule to the spectrum of the whole mixture.

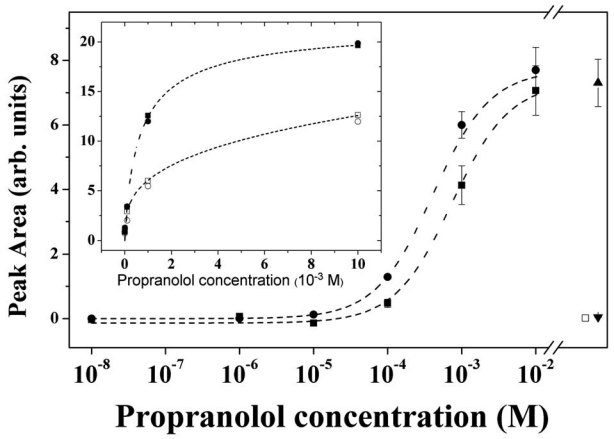

FIG. 5. Binding of ligand to *R*-propanolol MIP. Solid circles denote *R*-propanolol (the original MIP template) and solid squares denote *S*-propanolol (enantiomer). The data is presented after subtraction of nonspecific binding, as determined from an identical experiment with NIP. The rightmost points (to the right of the axis break) are not part of the same experiment and are plotted for comparison: up-pointing triangle denote MIP as imprinted, down-pointing triangle denote extracted MIP and open square denote NIP. The selectivity of the MIP in favor of the original template molecule peaks around $10^{-3}M$. Error bars represent ±SEM. Dotted lines represent fitting to Langmuir equation. Inset: solid circles and squares denote original MIP data (*R*- and *S*-propranolol, respectively) and corresponding NIP (open circles and squares, respectively).

Three such peaks (at 736.1, 1385.2, and 1582.3 cm^{-1}) are identified in Fig. 2 and marked with vertical dashed lines.

We then measured the spectra of MIP as imprinted and of extracted MIP, and compared them to the spectra of a NIP and of the template molecule. The three characteristic peaks of propranolol, already identified in Fig. 2, are marked with vertical dashed lines in Fig. 3. The spectra (a)–(c) were normalized according to the height of the peak at 2935 cm^{-1}, contributed by the polymer mixture [as obvious from the NIP spectrum, (c)]. The predominant peak in the spectrum of propranolol [Figs. 2(d) and 3(d)], in the 1380 cm^{-1} region, which is also clearly distinguishable in the spectrum of the mixture [Fig. 2(f)] and present in the polymerized MIP [Fig. 3(a)], decreases dramatically upon template extraction [Fig. 3(b)], rendering the spectrum of the extracted MIP almost identical to that of the NIP [Fig. 3(c)]. This peak was chosen for quantification of propranolol rebinding experiments. We note that this strong propranolol peak overlaps weaker peaks originating in other components of the mixture. Thus, to correctly account for the amounts of propranolol only, we deconvolute the broad peak in the 1380 cm^{-1} region into four Gaussian contributions, for both MIP and NIP. The deconvolution is presented in Fig. 4 where the leftmost peak's area represents the (relative) amount of propranolol.

Using this procedure, we quantified the amount of bound *R*-propranolol and *S*-propranolol by the *R*-propranolol imprinted MIP and the corresponding NIP, for a range of ligand concentrations. The specific binding was calculated by subtracting the value measured for NIP from the value measured for MIP, leading to the results presented in Fig. 5. Solid circles show the specific binding of *R*-propranolol by the MIP and solid squares show the specific binding of *S*-propranolol ("wrong" analyte) by the MIP. The three rightmost points are plotted for comparison and represent the amount of *R*-propranolol measured in the MIP immediately following polymerization (up-pointing triangle), the amount of *R*-propranolol measured in the MIP following template elution (down-pointing triangle) and NIP (open square). We also fit Langmuir binding isotherm equations to the data representing binding of *R*- and *S*-propranolol to the MIP, and plot them as dashed lines in the main plot of Fig. 5. The dissociation constants we extract are 0.4 and 1 mM for *R*-propranolol (the imprinted target) and its enantiomer, respectively, demonstrating the MIP selectivity.

We have detected and quantified the binding of the imprinting template in MIP using Raman microspectroscopy over a broad concentrations range. The confocal setup facilitated acquisition of measurements from volumes as small as $\sim 1\ \mu m^3$. We showed that the method is highly specific and appropriate for use as a label-free detection method. Most encouraging is the fact that precise quantification of the bound template is possible, based on one predominant peak in the Raman spectrum contributed by the target molecule. This suggests that in future applications, the reading can be very fast, by limiting the acquisition range to the relevant peak region only. Although the method is clearly less sensitive than radioligand assays, it is anticipated that surface enhanced Raman spectroscopy will provide even higher sensitivities, holding the promise of a specific, sensitive and rapid label-free detection method for nanostructures of MIPs.

A-S.B., K.H., and L.A.G. gratefully acknowledge financial support from the European Union (MENDOS project, Grant No. QLK4-CT2002-02323, Marie Curie Research Training Network NASCENT, Grant No. MRTN-CT-2006-33873). I.B. thanks the James Franck Binational German–Israeli Program in Laser–Matter Interaction.

[1] R. Arshady and K. Mosbach, Makromol. Chem. **182**, 687 (1981).
[2] G. Wulff and A. Sarhan, Angew. Chem., Int. Ed. **11**, 341 (1972).
[3] S. C. Zimmerman and N. G. Lemcoff, Chem. Commun. **2004**, 5.
[4] K. Haupt, Chem. Commun. **2003**, 171.
[5] V. Espina, A. I. Mehta, M. E. Winters, V. Calvert, J. Wulfkuhle, E. F. Petricoin, and L. A. Liotta, Proteomics **3**, 2091 (2003).
[6] A. Lueking, D. J. Cahill, and S. Mullner, Drug Discovery Today **10**, 789 (2005).
[7] M. Lynch, C. Mosher, J. Huff, S. Nettikadan, J. Johnson, and E. Henderson, Proteomics **4**, 1695 (2004).
[8] K. K. Jain, Curr. Opin. Drug Discovery Dev. **7**, 285 (2004).
[9] A.-S. Belmont, M. Sokuler, K. Haupt, and L. A. Gheber, Appl. Phys. Lett. **90**, 193101 (2007).
[10] F. Vandevelde, T. Leïchlé, C. Ayela, C. Bergaud, L. Nicu, and K. Haupt, Langmuir **23**, 6490 (2007).
[11] M. Jakusch, M. Janotta, B. Mizaikoff, K. Mosbach, and K. Haupt, Anal. Chem. **71**, 4786 (1999).
[12] St. Kostrewa, M. Emgenbroich, D. Klockow, and G. Wulff, Macromol. Chem. Phys. **204**, 481 (2003).
[13] R. H. Uibel and J. M. Harris, Anal. Chem. **77**, 991 (2005).
[14] D. McStay, A. H. Al-Obaidi, R. Hoskins, and P. J. Quinn, J. Opt. A, Pure Appl. Opt. **7**, S340 (2005).
[15] L. I. Andersson, Anal. Chem. **68**, 111 (1996).
[16] R. H. Schmidt and K. Haupt, Chem. Mater. **17**, 1007 (2005).